Available online at www.sciencedirect.com
ScienceDirect
Journal of Hazardous Materials 150 (2008) 494–503
Journal of Hazardous Materials
www.elsevier.com/locate/jhazmat

Effects of synthesis temperature on the microstructures and basic dyes adsorption of titanate nanotubes

Chung-Kung Lee [a], Kuen-Song Lin [b,*], Chian-Fu Wu [b], Meng-Du Lyu [a], Chao-Chun Lo [b]

[a] *Green Environment R&D Center and Department of Environmental Engineering, Vanung University, Chung-Li 32061, Taiwan, ROC*
[b] *Department of Chemical Engineering and Materials Science/Fuel Cell Center, Yuan Ze University, Chung-Li, Taiwan 32061, Taiwan, ROC*

Received 9 February 2007; received in revised form 28 April 2007; accepted 30 April 2007
Available online 5 May 2007

Abstract

The adsorption of two basic dyes (Basic Green 5 (BG5) and Basic Violet 10 (BV10)) onto titanate nanotubes (TNT) that were prepared via a hydrothermal method with different synthesis temperatures was studied to examine the potential of TNT for the removal of basic dyes from aqueous solution. Effects of synthesis temperature on the microstructures of TNT were characterized with transmission electron microscopy (TEM), X-ray diffraction (XRD), and nitrogen adsorption–desorption isotherms. For synthesis temperature greater than 160 °C, the microstructure of titanate might transform from nanotube into nanorod accompanying with the sharp decrease in the titanate interlayer spacing, BET surface area, and pore volume. Effects of the pore structure variation on the basic dyes adsorption of TNT were discussed. Moreover, the adsorption mechanisms of basic dyes from aqueous solution onto TNT were examined with the aid of model analyses of the adsorption equilibrium and kinetic data of BG5 and BV10. The regeneration of TNT was also briefly discussed.

Keywords: Titanate nanotubes; Synthesis temperature; Nanorod; Basic dyes; Adsorption

1. Introduction

The synthesis of nanotubes has become one of the most important research subjects in nanotechnology and various nanotubular materials have been produced during the last decades [1,2]. The success of preparing titania nanotubes is one of the examples of such intense research efforts. During 1998–1999, Kasuga et al. [3,4] reported the preparation of TiO_2-derived nanotubes by a hydrothermal treatment of TiO_2 powder in a 10 M NaOH aqueous solution with different reaction temperature and time. This method does not require any templates and the obtained nanotubes have small diameter of ca. 10 nm and high crystallinity. Many groups have tried to analyze the characteristics of TNT, from which the synthetic mechanism was examined and the sheet folding mechanism was often assumed [5,6]. The effects of synthetic conditions on the microstructures of the TiO_2-derived nanotubes were also investigated, with the emphasis placed on the reaction time, calcination temperature, and acid washing concentration [7–10]. However, it is hardly found in the literature to investigate systematically the effects of synthesis temperature on the microstructures of TNT although it also plays a key factor in the hydrothermal method [11].

Dye wastewaters are recognized as difficult-to-treat pollutants and discharged by a wide variety of sources, such as textiles, printing, dyeing, dyestuff manufacturing, and food plants [12]. The color produced by minute amounts of organic dyes in water is of great concern because the color in water is aesthetically unpleasant. Moreover, they are also the important sources of water pollution, because some dyes and their degradation products may be carcinogens and toxic to human beings or mammals. Some investigations have been conducted on the physical, chemical, and biological methods for removal of the color from dye wastewater [13–17] and it was found that physical adsorption might be an efficient and economic process to remove dyes from the wastes streams and also to control the biochemical oxygen demand [18]. The application of adsorption technology utilizing commercial activated carbon has become known and taken a place as one of the most effective technologies for the removal of effluents of dyes [19]. However, activated carbon often suffers from high-cost production and regeneration

* Corresponding author. Tel.: +886 34638800x2574; fax: +886 34559373.
E-mail address: kslin@saturn.yzu.edu.tw (K.-S. Lin).

0304-3894/$ – see front matter © 2007 Elsevier B.V. All rights reserved.
doi:10.1016/j.jhazmat.2007.04.129

and other materials, such as some natural adsorbents, certain waste materials, and some agricultural by-products, are alternatives [20–22]. In recent years, mesoporous molecular sieves, such as FSM-16 [23], MCM-22 [24], and MCM-41 [25,26], have been accepted as the appropriate adsorbents for the removal of dyes from wastewater due to their unique mesoporous pore structure characterized by high specific surface area and pore volume. Because TNT derived from hydrothermal method possess ion-exchange property [7,9] and are also characterized by high surface area and pore volume [10], they may also offer a special environment for the adsorption of large cations, such as basic dyes. Moreover, the hydrothermal method above mentioned is also a simple, cost-effective, and environmentally friendly technology and can prepare high-yield TNT. Therefore, it may be an important task to examine the potential applications of TNT that is synthesized from such a method in the environmental protection. In this study, the objectives are to examine the effects of synthesis temperature of hydrothermal method on the morphology, phase structure, and pore structure of TNT as well as the potential of TNT for the adsorptive removal of basic dyes from wastewater. The relationship between the alteration in the microstructure induced by the variation of synthesis temperature and the change in the basic dyes adsorption capacity of TNT is discussed. The thermodynamic and kinetic parameters of BG5 and BV10 adsorption are calculated to examine the adsorption mechanisms of basic dyes from water solution onto the TNT. The regeneration of TNT is also briefly discussed.

2. Materials and methods

2.1. Preparation of TNT

TNT was prepared using a hydrothermal process similar to that described by Kasuga et al. [3,4]. TiO_2 source used for the TNT was commercial-grade TiO_2 powder (from Sigma–Aldrich, 99.999% purity) with crystalline structure of ca. 25% rutile and ca. 75% anatase and primary particle size of ca. <50 nm. In a typical preparation, 1–3 g of the TiO_2 powder was mixed with 60–90 mL of 10 M NaOH solution followed by hydrothermal treatment of the mixture at 110–270 °C in a 250 mL teflon-lined autoclave for 24 h. After hydrothermal reaction, the precipitate was separated by filtration and washed with a 1 M HCl solution and distilled water until the pH value of the rinsing solution reached ca. 7.0, approaching the pH value of the distilled water. The acid washed samples were dried in a vacuum oven at 110 °C for 8 h and stored in the glass bottles until used.

2.2. Characterization of TNT

TEM analyses were conducted to investigate the morphologies and microstructures of the TNT samples with a H-7500 electron microscope (Hitachi, Japan), using 120 kV accelerating voltage. Energy dispersive X-ray (EDX) spectra were obtained with a S-4000 scanning electron microscopy (Hitachi, Japan), using 25 kV accelerating voltage. XRD patterns scanned from 5° to 70° with a scan rate of 4°/min were obtained on a thermal ARL X-ray diffractometer (Thermo, France) equipped with a Cu Kα radiation source and a graphite monochromator and were used to determine the identity of any crystalline phase or structures in the TNT samples. The porous structure characteristics, including the BET surface area, the pore volume, and the pore size distribution, were obtained from the conventional analysis of nitrogen isotherms measured at 77 K with Micromeritics TriStar 3000 apparatus. All the samples were degassed at 100 °C prior to the measurement.

2.3. Adsorption study

Two basic dyes (BG5 and BV10) were selected as adsorbates to discuss the adsorption selectivity of TNT in terms of pore structure of adsorbent and molecular shape of adsorbates. The chemical structures of the examined dyes were shown in Fig. 1. The two compounds were of analytical grade from Sigma Chemical Co. (USA) and were used without further purification. The basic dyes adsorption data from aqueous solution were obtained by the immersion method. BG5 and BV10 were first dried at 105 °C for 24 h to remove the moisture before use. All of the dye solutions were prepared with distilled water. For adsorption experiments, 0.1-g-TNT was added into 100 mL of dye aqueous solutions at the desired concentrations. The initial pH value of the solution was adjusted with NaOH or HCl solution to reach a desirable value. The preliminary experiment revealed that about 3 h was required for the adsorption process to reach equilibrium with a reciprocating shaker equipped with a constant temperature controller and a cover to keep isothermal condition. The solution and solid phase were separated by the centrifugation at 8000 rpm for 25 min in a Sorvall RC-5C centrifuge. A 15-mL aliquot of the supernatant was taken and analyzed for BG5 and BV10 by UV–vis spectrophotometer (UV-160A, Shimadzu) at

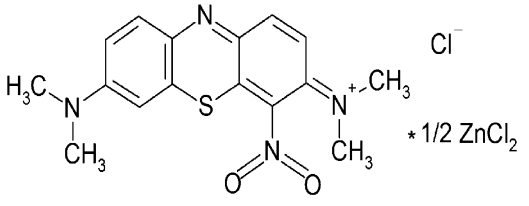

BG5

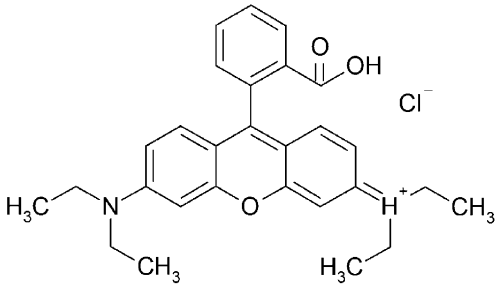

BV10

Fig. 1. Chemical structures of the examined dyes.

the wave length of 655 and 555 nm, respectively. The adsorption capacity of dyes was then calculated using the relation $Q = V\Delta C/m$, where V was the volume of the liquid phase, m was the mass of TNT, and ΔC was the difference between the initial and final concentration of dye at solutions, which could be computed simply from the initial and final UV readings. For the adsorption kinetics experiments, the dye adsorption amounts were determined by analyzing the solution at appropriate time intervals. The effects of temperature on the adsorption data were carried out by performing the adsorption experiments at various temperatures (25, 35, and 45 °C).

In this study, the adsorption mechanism of BG5 and BV10 from water solution onto TNT surfaces was first examined with the aid of the Dubinin–Kaganer–Radushkevick (DKR) equation. The DKR equation had the following form:

$$\ln\ Q = \ln\ Q_{\mathrm{m}} - \beta\varepsilon^2 \tag{1}$$

where Q was the adsorption amount of BG5 and BV10 in mol g^{-1}, Q_{m} (mol g^{-1}) the DKR monolayer capacity, β (mol^2 J^{-2}) a constant related to sorption energy, and ε was the Polanyi potential which was related to the equilibrium concentration as

$$\varepsilon = RT\ \ln\left(\frac{1}{C}\right) \tag{2}$$

where T was the temperature and C was the equilibrium concentration of BG5 and BV10 [22,27]. The slope and intercept of the plots of $\ln Q$ versus ε^2 give β and Q_{m}, respectively. The value of β was related to the sorption energy, E, via the following relationship:

$$E = \frac{-1}{\sqrt{-2\beta}} \tag{3}$$

Moreover, since the adsorption isotherms have been measured at three temperatures, the heat of adsorption can be calculated. The temperature dependency of adsorption equilibrium constant K (*i.e.*, amount of removed basic dyes per gram of TNT divided by basic dyes concentration in the liquid phase) obeyed the van't Hoff equation:

$$\frac{\mathrm{d}\ \ln\ K}{\mathrm{d}T} = \frac{\Delta H}{RT^2} \tag{4}$$

where R was the gas constant and T was the temperature (in K). Eq. (4) could be integrated to yield $\ln K = \ln K_0 + (-\Delta H/RT)$. A plot of $\ln K$ versus $1/T$ will yield a straight line with a slope of $-\Delta H/R$ [28].

For the kinetic data, a simple kinetic analysis was performed with the aid of pseudo-second-order equation [29]. In this equation, the value of the rate constant k could be calculated in the form

$$\frac{\mathrm{d}Q_t}{\mathrm{d}t} = k(Q_{\mathrm{e}} - Q_t)^2 \tag{5}$$

where Q_{e} and Q_t were the amount of dye adsorbed per unit mass of the adsorbent at equilibrium and time t, respectively. After definite integration by applying the initial conditions $Q_t = 0$ at $t = 0$ and $Q_t = Q_t$ at $t = t$, Eq. (5) became

$$\frac{t}{Q_t} = \frac{1}{kQ_{\mathrm{e}}^2} + \frac{1}{Q_{\mathrm{e}}}t \tag{6}$$

In addition to the pseudo-second-order rate equation, the intraparticle diffusion model was commonly used for examining the steps involved during adsorption, described by external mass transfer (boundary layer diffusion) and intraparticle diffusion [24]. The intraparticle diffusion model was expressed as

$$Q_t = k_{\mathrm{d}}t^{1/2} \tag{7}$$

where k_{d} was the diffusion coefficient. If the double nature of intraparticle diffusion plot confirmed the presence of a boundary-layer effect and pore diffusion, the adsorption kinetic data could be further analyzed using the Boyd kinetic expression (Eq. (8)) to determine the actual rate-controlling step involved in the dye adsorption process [30]

$$G = 1 - \frac{6}{\pi^2}\exp\left(-Bt\right) \tag{8}$$

$$B = \frac{\pi D}{r^2} = \text{time constant} \tag{9}$$

where D was the effective diffusion coefficient of adsorbates in adsorbent phase, r the radius of adsorbent particle assumed to be spherical, and G was the fraction of solute adsorbed at different times t and given by

$$G = \frac{Q_t}{Q_{\mathrm{e}}} \tag{10}$$

where Q_t and Q_{e} represented the amount adsorbed (mol g^{-1}) at time t and at infinite time. In this work, we took the Q_{e} from the pseudo-second-order kinetic model. Substituting Eq. (10) into Eq. (8), the kinetic expression became

$$Bt = -0.4977 - \ln\left(1 - \frac{Q_t}{Q_{\mathrm{e}}}\right) \tag{11}$$

In general, if the plot of Bt versus t was a straight line passing through the origin, the adsorption was governed by a particle-diffusion mechanism, otherwise it was governed by film diffusion [31].

3. Results and discussion

3.1. Morphology of TNT

Fig. 2 shows the TEM images of titanate compounds obtained by a hydrothermal reaction using commercial-grade TiO_2 powder and 10 M NaOH aqueous solution as precursors at 120, 150, 240, and 270 °C for 24 h. A large amount of TNT with a diameter of 10–30 nm and a length of several hundreds nanometers are obtained. Further observation indicates that the prepared titanate compounds possess uniform inner and outer diameters along their length as well as multi-layered and open-ended, in good agreement with the previous reports [7,9,10].

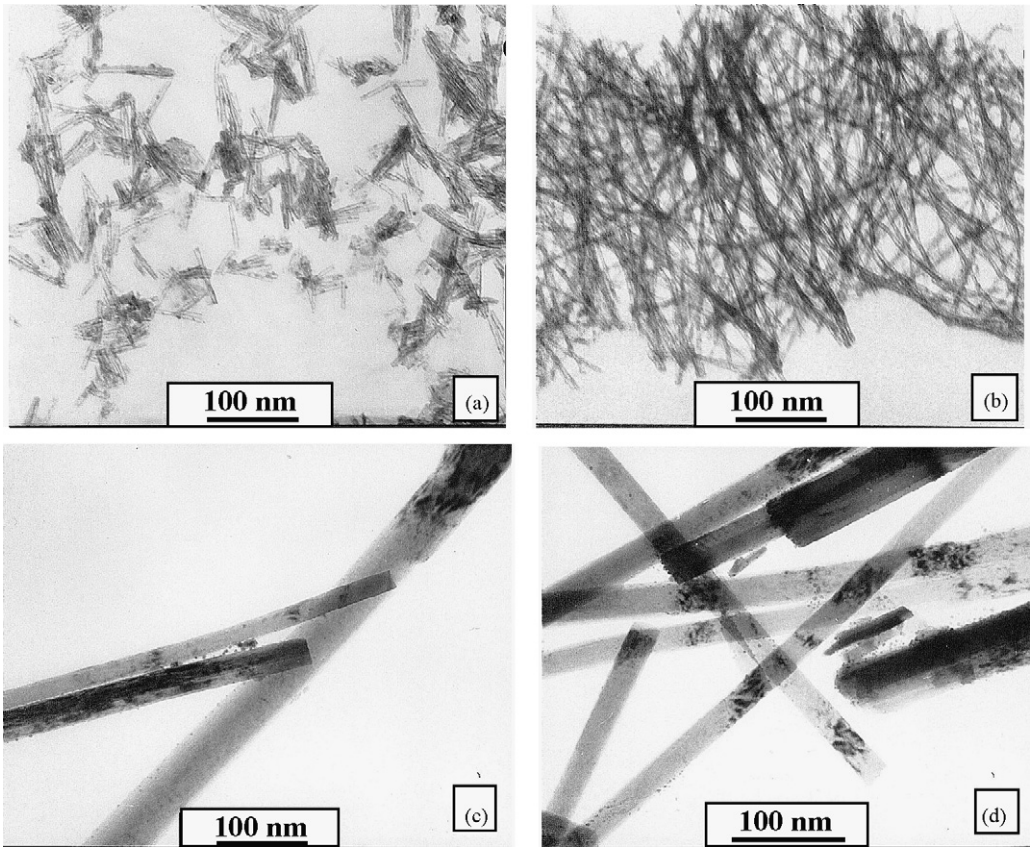

Fig. 2. TEM micrographs of the titanate products obtained by hydrothermal process at (a) 120 °C, (b) 150 °C, (c) 240 °C, and (d) 270 °C for 24 h.

3.2. XRD patterns

Fig. 3 shows the XRD patterns of the samples synthesized at 110–180, 210, and 270 °C for 24 h. It is evident from Fig. 3 that the XRD patterns corresponding to synthesis temperatures below and above 160 °C are distinct, indicating that synthesis temperature may induce a significant change in the phase structure of titanate compounds. The characteristic peak at around $2\theta = 10^\circ$ for all XRD patterns indicates that the samples are composed of a layered titanate. Moreover, because the reflection peak at $2\theta = 10^\circ$ corresponds to the interlayer spacing of the samples, the peak shifting gradually to higher angles for temperatures greater than 160 °C means the decrease of the interlayer spacing [7].

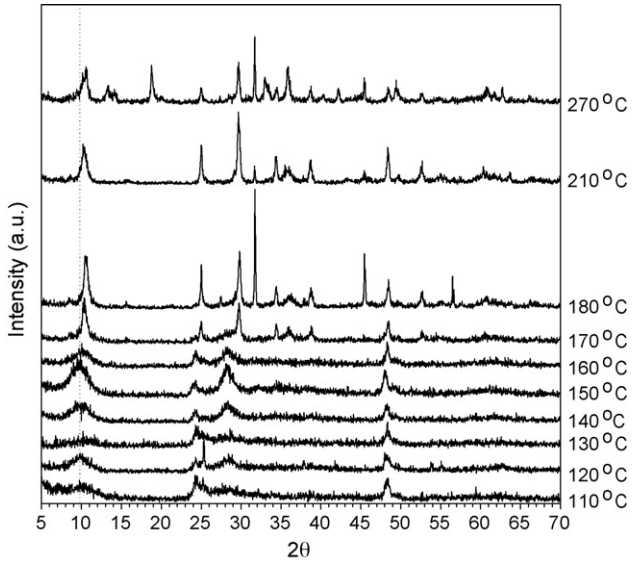

Fig. 3. XRD patterns of the titanate products obtained by hydrothermal process at 110–270 °C for 24 h.

For temperatures ≤160 °C, the XRD patterns are not changed so drastically with the variation of temperature. There is a broad peak from $2\theta = 23^\circ$ to 25°, which can be assigned to hydrogen titanate compounds according to the standard XRD data. Moreover, there exists a diffraction peak around $2\theta = 48.4^\circ$ besides the weak peak from $2\theta = 23^\circ$ to 25°, which may be ascribed to sodium titanate compounds [7,9]. As reported in the literature, the sodium titanates are probably first formed from original titania powder through hydrothermal treatment, and then the sodium titanate products change to hydrogen titanate after washing in acidic solution through an ion-exchange mechanism [9]. Moreover, the crystal structure of the TiO_2-derived titanates is similar to that of $H_2Ti_3O_7$ ($Na_2Ti_3O_7$), $Na_xH_{2-x}Ti_3O_7$, $H_xTi_{2-x/4\ x/4}O_4$ ($x = 0.75$), $Na_2Ti_2O_4(OH)_2$, or $Na_yH_{2-y}Ti_nO_{2n+1}\cdot xH_2O$, probably due to their same layered titanate family [32]. In this study, EDX analysis demonstrates the existence of sodium ions in the synthesized nanotubes (not shown here). Therefore, it can be concluded that the sodium ions are not substituted completely by protons after the nanotubes are washed with the HCl aque-

ous solution and the distilled water. Moreover, TGA curve (not shown here) shows that a mass loss of ca. 11% is observed after the nanotubes are heated from room temperature to 1200 °C. Considering the existence of Na^+ in the nanotubes, a large mass loss during heat-treatment, and the XRD patterns, the synthesized titanate compounds at temperatures lower than 160 °C may be described as trititanate $(H,Na)_2Ti_3O_7{\cdot}xH_2O$ [7,8].

For higher temperatures than 160 °C, the XRD patterns are very different from that of samples synthesized at temperatures ≤160 °C, showing that there are significant changes on the microstructure of titanate samples. It has been reported that the titania nanotubes might be formed from hydrogen titanate nanotubes by heat treating at 400 °C [9,10]. Moreover, it was also demonstrated that for TNT with the post-heat-treatment above 350 °C, some of the nanotubes began to break into particles of anatase phase, and the others remained as nanotubes where a lot of Na^+ existed, indicating that the remnant Na atoms stabilized the nanotube structures [7]. As shown in Fig. 3, there is a broad peak at $2\theta = 25°$ for synthesis temperatures greater than 160 °C, indicating the existence of anatase-type TNT. The other obvious peaks shown in Fig. 3 may be assigned to the sodium hexatitanate, $Na_2Ti_6O_{13}$ [7]. Moreover, because the interlayer spacing of samples synthesized at temperatures >160 °C is smaller than that of samples synthesized at temperatures ≤160 °C, the TNT may change into thick sodium titanate nanorods when the synthesis temperatures are greater than 160 °C, as can be further verified with the analysis of BET surface area and pore volume.

3.3. BET surface area and pore volume

Fig. 4 shows some nitrogen adsorption–desorption isotherms measured on the prepared titanate samples. Some key features

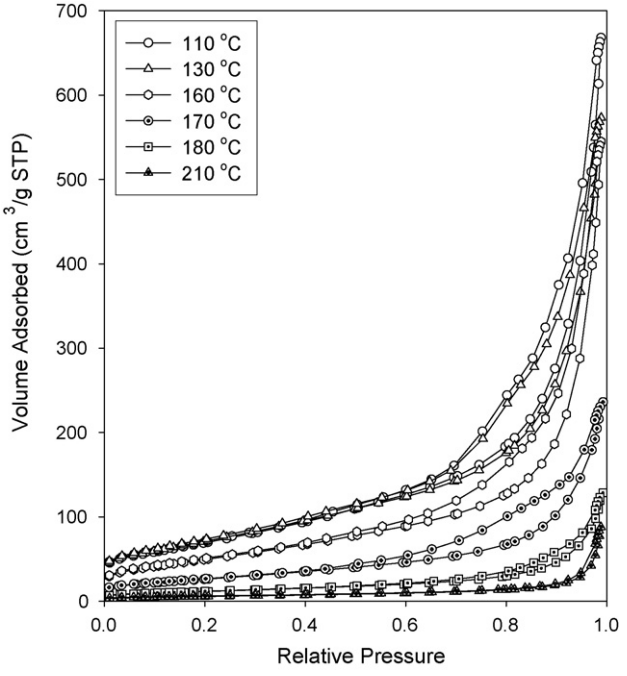

Fig. 4. Nitrogen adsorption–desorption isotherms of the titanate products obtained by hydrothermal process at 110, 130, 160, 170, 180, and 210 °C for 24 h.

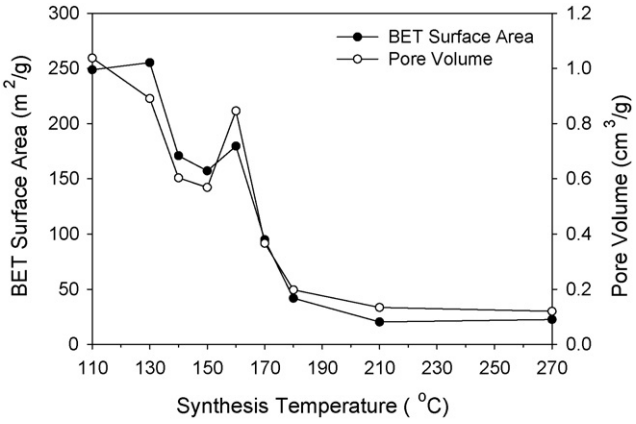

Fig. 5. BET surface area and pore volume of the titanate products obtained by hydrothermal process at 110–210 °C for 24 h.

may be found directly from this figure. It can be seen that the monolayer capacity, thus the BET surface area of titanate samples, becomes smaller when the synthesis temperature increases, especially as temperatures are greater than 160 °C. A more clear dependence of BET surface area on the synthesis temperature is shown in Fig. 5. As discussed in the XRD patterns, when the temperatures are greater than 160 °C, the interlayer spacing of titanates decrease and the nanotubes may change into thick nanorods, introducing a sharp decrease in the BET surface area.

Moreover, all adsorption isotherms presented in Fig. 4 are typically BDDT type II in shape [33] and a large uptake is observed when close to saturation pressure, where capillary condensation in the large voids among the aggregates of TNT starts. Because the saturation adsorption capacity of nitrogen corresponds to the pore volume of titanate samples, the isotherms shown in Fig. 4 also suggest that the pore volume will decrease as the synthesis temperature increases. This result is similar to the effects of synthesis temperature on the BET surface area (see Fig. 5), namely, the increase of synthesis temperature will decrease the BET surface area and the pore volume of TNT simultaneously.

The nitrogen isotherms of all titanate samples in Fig. 4 also show a clear hysteresis loop, indicating the presence of mesopores (2–50 nm). On the other hand, for the increase of synthesis temperature, the hysteresis loops shift to the region of higher relative pressure and the areas of the hysteresis loops gradually become small. When the temperatures are greater than 180 °C, the hysteresis loop of the samples is difficult to be observed. Fig. 6 shows the corresponding pore size distributions of the titanate samples synthesized with different temperatures. It can be seen that the pore size distributions of the titanate samples strongly depend on the synthesis temperature. Considering the morphology of the titanate samples observed in Fig. 2, the smaller pores (<10 nm) may correspond to the pores inside the TNT and the diameters of these pores are equal to the inner diameter of the nanotubes, while the larger pores (10–100 nm) can be attributed to the voids in the aggregation of the nanotubes [10]. As can be seen from Fig. 6, for synthesis temperatures greater than 160 °C, the smaller pores (<10 nm) disappear due to the formation of thick titanate nanorods.

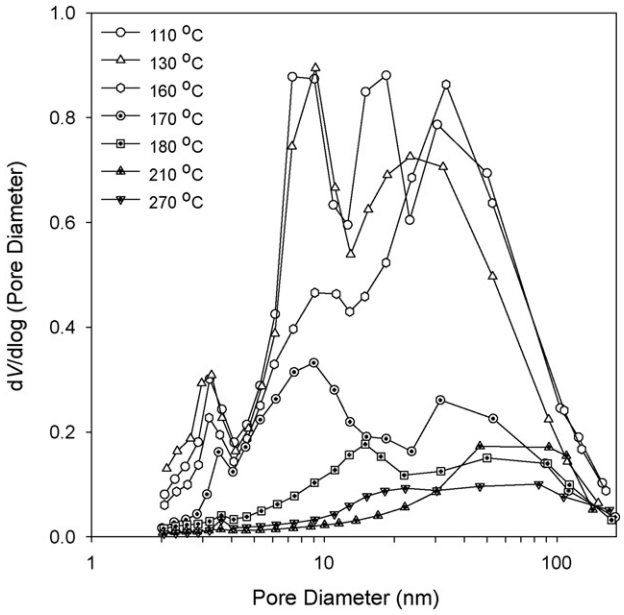

Fig. 6. Pore size distribution curves of the titanate products obtained by hydrothermal process at 110, 130, 160, 170, 180, 210, and 270 °C for 24 h.

According to the above results, it can be concluded that when the synthesis temperature is greater than 160 °C, the microstructure of titanate samples may be transformed from nanotube into nanorod accompanying with the decrease of titanate interlayer spacing, BET surface area, and pore volume. Because the TNT possesses ion-exchange property and mesoporous structure, it may be a good adsorbent for the removal of basic dyes with the ion-exchange mechanism, especially for the samples prepared at low synthesis temperatures (such as 110–160 °C), which are characterized with high BET surface area and pore volume.

3.4. Effects of synthesis temperature on the basic dyes adsorption capacity of TNT

Fig. 7 shows the effects of synthesis temperature on the adsorption capacity of titanate samples for BG5 and BV10. The adsorption data are measured at 25 °C with an initial dye concentration of 2000 mg/L. It is found that for synthesis temperatures ≤160 °C, the adsorption capacity increases with the increasing temperature and reaches the maximum at 160 °C for both BG5 (211 mg/g) and BV10 (118 mg/g). This tendency is not completely consistent with the relationship between the BET surface area and synthesis temperature. In general, the adsorption of basic dyes onto titanate samples is a cation exchange mechanism and the dominating factors controlling the adsorption capacity are the cation exchange capacity and the pore volume of titanate samples. Because the pore volume of titanate samples decreases with the increasing synthesis temperature, the above results imply that the increasing synthesis temperature may induce an increase in the cation exchange capacity of titanate samples. For synthesis temperatures greater than 160 °C, the adsorption capacity decreases sharply and becomes very low as temperatures are greater than 170 °C. This result may be ascribed to the microstructure change from nanotube into nanorod and the accompanying fast decrease in the pore volume of titanate samples. On the other hand, if we compare the adsorption capacity of BG5 and BV10, it can be seen that the adsorption capacity of BG5 is greater than that of BV10 in all examined samples. This may be ascribed to the smaller size of BG5 and then the more efficient packing array of BG5 in TNT [15]. Finally, it should be noteworthy that the adsorption capacity of BG5 on the TNT synthesized at 160 °C is comparable to that of BG5 on the activated carbon (216 mg/g) [15]. However, the adsorption capacity of BV10 on the TNT is smaller than that of BV10 on the activated carbon (198 mg/g) [15]. The high adsorption capacity of BG5 on the TNT synthesized at 160 °C indicates that TNT may be a good adsorbent for the removal of basic dyes from wastewater if the synthesis temperature is appropriately selected.

The XRD patterns accompanied with the dyes adsorption process are demonstrated in Fig. 8. If the diffraction patterns are compared, it is clearly observed that the adsorption of BG5 may induce some disorders on the layered structure of TNT, as indicated by the almost disappearance of diffraction peak at

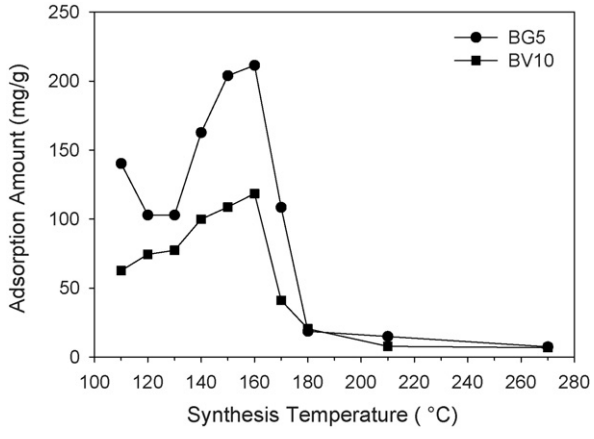

Fig. 7. Adsorption capacity of BG5 and BV10 measured at initial dyes concentration of 2000 mg/L, pH 4, and 25 °C on the titanate products obtained by hydrothermal process at 110–270 °C for 24 h.

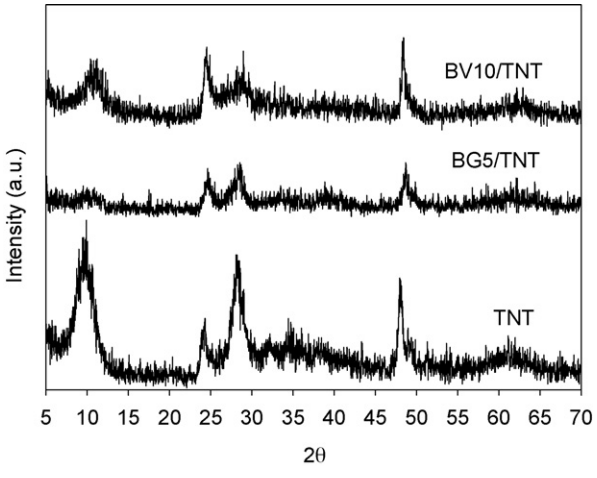

Fig. 8. XRD patterns of the titanate products (synthesized at 160 °C) before and after adsorbing BG5 and BV10.

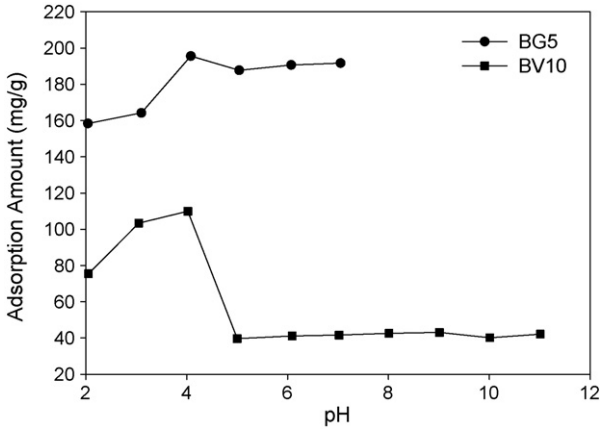

Fig. 9. Effect of pH on the basic dyes adsorption onto TNT at 25 °C and dye initial concentration 900 mg/L.

$2\theta = 10^{\circ}$. This result may be ascribed to the dense packing of BG5 in the TNT. For BV10 adsorption, the decrease of titanate interlayer spacing during the adsorption processes is evidenced with the characteristic peak of layered titanate moving to higher angle.

The pH value of the aqueous solution is an important controlling parameter in the adsorption process, as characterized in Fig. 9. For BG5, the adsorption capacity is measured under pH < 8, because it may decompose when pH > 8. As demonstrated in Fig. 9, pH value will affect the adsorption behavior of TNT and the adsorption capacity of BG5 and BV10 decreases significantly at the pH values of 2–3 and 5–11, respectively. Since the adsorption capacities of both BG5 and BV10 are high at pH 4, pH 4 is adopted in the measurements of adsorption isotherms and adsorption kinetic data of BG5 and BV10.

In the following, the discussion of the adsorption isotherms and kinetics of both BG5 and BV10 on TNT synthesized at 160 °C for providing more information about the adsorption mechanisms of basic dyes from water solution onto TNT is given.

3.5. Adsorption isotherms of BG5 and BV10

Fig. 10 shows the BG5 and BV10 adsorption isotherms at different temperatures. As can be seen from this figure, the adsorption capacity of basic dyes on TNT is susceptible to temperature changes and the isotherm types can be divided into two cases: type I (BG5) and type V (BV10) [33]. As mentioned earlier, the adsorption of both BG5 and BV10 may introduce some disorders in the pore structure of TNT. Therefore, the change in the adsorption isotherm type may be closely related to the effect of basic dyes adsorption on the pore structure stability of TNT. In the following, the adsorption mechanism of BG5 and BV10 from aqueous solution onto TNT surfaces is first examined with the aid of the DKR equation. The DKR parameters and E values for the adsorption of BG5 and BV10 onto TNT are presented in Table 1. The correlation coefficients (r^2) for the linear regression analysis are close to unity. As shown in Table 1, the E values are found to be −15.95 (−8.59), −13.85 (−8.47), and −13.03 (−8.28) kJ mol^{-1} for BG5 (BV10) adsorption at

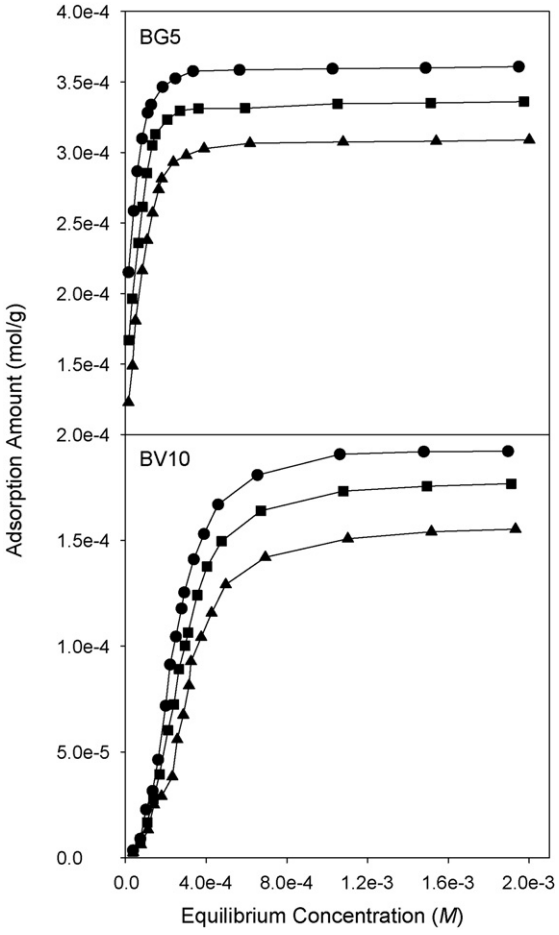

Fig. 10. Adsorption isotherms of BG5 and BV10 on TNT at different temperatures and pH 4. (●) 25 °C, (■) 35 °C, and (▲) 45 °C.

25, 35, and 45 °C, respectively. As expected, these values are of the order of an ion-exchange mechanism, in which the sorption energy lies within 8–16 kJ mol^{-1} [27,34]. Moreover, the dependence of adsorption capacity Q_m on the temperature and adsorbate is inconsistent with the adsorption isotherms shown in Fig. 10, which may be due to the fact that the DKR equation is apparently obeyed in a lower concentration range [27].

As shown in Fig. 10, the concentration of the adsorbed BG5 and BV10 decreases with the increased temperature at a given equilibrium concentration and the adsorption is an exothermic process. The heats of adsorption, calculated from the van't Hoff equation, are -33.9 ± 0.5 and -28.4 ± 7.4 kJ mol^{-1} for BG5 and BV10, respectively.

Table 1
DKR parameters and E values of BG5 and BV10 adsorption onto TNT

T (°C)	Dye	Q_m (mol g^{-1})	β (mol^2 J^{-2})	E (kJ mol^{-1})
25	BG5	8.91×10^{-4}	-1.97×10^{-9}	−15.95
35		1.18×10^{-3}	-2.61×10^{-9}	−13.85
45		1.32×10^{-3}	-2.94×10^{-9}	−13.03
25	BV10	1.83×10^{-3}	-6.78×10^{-9}	−8.59
35		2.07×10^{-3}	-6.96×10^{-9}	−8.47
45		3.43×10^{-3}	-7.30×10^{-9}	−8.28

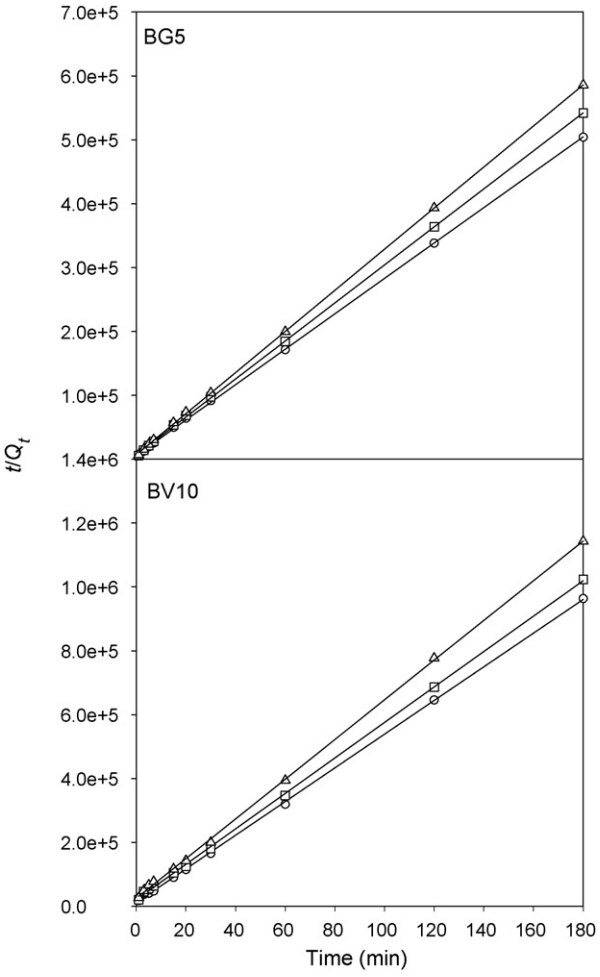

Fig. 11. Comparison of pseudo-second-order kinetics of BG5 and BV10 adsorption onto TNT. Conditions: initial dyes concentration 900 mg/L and pH 4. (◯) 25 °C, (□) 35 °C, and (△) 45 °C.

3.6. Adsorption kinetics of BG5 and BV10

The effect of contact time on the amount of BG5 and BV10 adsorbed onto TNT is measured at the optimum initial concentration and different temperatures. A simple kinetic analysis is performed with the aid of pseudo-second-order equation (Eq. (6)). Linear plots of the t/Q_t versus t with linear regression coefficients higher than 0.999 indicates the applicability of this kinetic equation and the pseudo-second nature of the adsorption process of two basic dyes onto TNT (see Fig. 11). Table 2 lists the kinetic parameters obtained from the pseudo-second-order model and it is seen that the equilibrium adsorption capacity (Q_e) shows a slight decrease with the increasing temperature. From the k values it is observed that for BG5 and BV10, temperature effect on the adsorption kinetics is insignificant.

Fig. 12 presents the typical plots for the adsorption of BG5 and BV10 on TNT using the diffusion model (Eq. (7)). As shown in Fig. 12, the two-phase plot suggests that the adsorption process proceeds by surface adsorption and intraparticle diffusion, namely, the initial curved portion of the plot indicates a boundary-layer effect while the second linear portion

Table 2
Parameters of kinetic model of BG5 and BV10 adsorption onto TNT

T (°C)	Dye	Pseudo-second-order model		
		k (g/mol min)	Q_e (mol/g)	r^2
25	BG5	1285.4	3.61×10^{-4}	0.999
35		1339.8	3.36×10^{-4}	0.999
45		1475.3	3.11×10^{-4}	0.999
25	BV10	1820.4	1.90×10^{-4}	0.999
35		1514.5	1.80×10^{-4}	0.999
45		1542.3	1.61×10^{-4}	0.999

Conditions: initial dye concentration 900 mg/L and pH 4.

is due to intraparticle or pore diffusion. Because the double nature of intraparticle diffusion plot confirms the presence of a boundary-layer effect and pore diffusion, the adsorption kinetic data can be further analyzed using Boyd kinetic expression (Eq. (8)) to determine the actual rate-controlling step involved in the dye adsorption process. Fig. 13 shows the calculated Bt values against t for BG5 and BV10 at 25 °C. From Fig. 13, it is evident that the plots are not straight lines to pass the origin, implying

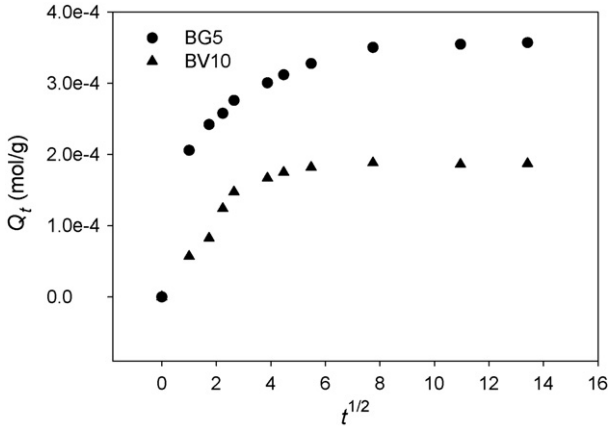

Fig. 12. The diffusion model plots for the adsorption of BG5 and BV10 on TNT. Conditions: initial dyes concentration 900 mg/L, 25 °C, and pH 4.

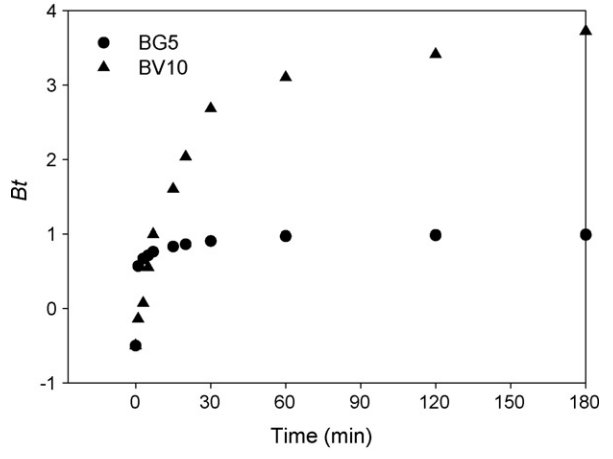

Fig. 13. Correlation between Bt and t for BG5 and BV10 adsorption onto TNT. Conditions: initial dyes concentration 900 mg/L, 25 °C, and pH 4.

external mass transport mainly governs the rate-limiting process. It is noteworthy that such type of pattern is also found for dyes adsorption on MCM-22 [24], rice husk [31], activated carbon [35], and fly ash [36].

As discussed in the above sections, TNT could be used as an effective adsorbent for basic dyes wastewater treatment. However, the regeneration of TNT is also an important issue in the TNT utilization. Currently, two major regeneration techniques have been used, namely, high temperature calcination for removal of organic and carbon deposits on adsorbents and ion-exchange regeneration for restoring the exchange capacity [37]. Recently, Fenton-driven oxidation has been proposed for regenerating spent organic-loaded carbons [38] and simple washing process with alkaline or acid solution has been proposed to recover the MCM-41 adsorbent and the adsorbed dyes [25]. For the regeneration of TNT, the high temperature calcination is inappropriate, because the heat-treating process has a significant effect on both the pore structure and surface chemical characteristics of TNT [10], which in turn results in an obvious decrease in their adsorption capacity for basic dyes. On the other hand, the simple washing process with alkaline or acid solution may be taken into consideration due to the fact that the adsorption of basic dyes onto TNT is closely related to the solution pH (especially, for BV10). Finally, it is well known that the as-prepared TNT may be used as an effective photocatalyst [39] and the photocatalytic degradation of the adsorbed basic dyes may also be used to the regeneration of TNT.

4. Conclusions

It was experimentally concluded that if the synthesis temperature was controlled at appropriate range (i.e., 150–160 °C) and the nanotubular structure of TNT could be well reserved during the hydrothermal process, TNT may be an effective adsorbent for basic dye removal from aqueous solutions. The adsorption capacity of BG5 on the TNT synthesized at 160 °C was comparable to that of BG5 on the activated carbon (216 mg/g). Solution pH will affect the adsorption behavior of TNT and the adsorption capacity of BG5 and BV10 decreases significantly at pH values of 2–3 and 5–11, respectively. Since the adsorption amount decreased as the temperature of the adsorption system was raised, the adsorption of basic dyes on TNT was an exothermic process. The adsorption isotherm types could be divided into two cases: type I (BG5) and type V (BV10), which might be closely related to the effect of basic dyes adsorption on the pore structure stability of TNT. Adsorption energy evaluated from DKR equation for the adsorption of BG5 and BV10 on TNT showed that an ion-exchange mechanism was operative. The heats of adsorption for BG5 and BV10 were estimated as −33.9 and −28.4 kJ/mol, respectively. The adsorption kinetics followed the pseudo-second-order model and the external diffusion was the controlling process. For the regeneration of TNT, both the simple washing with alkaline or acid solution and the photocatalytic degradation of the adsorbed basic dyes by using the TNT as photocatalysts may be taken into consideration.

References

[1] S. Sinnott, R. Andrews, Carbon nanotubes: synthesis, properties, and applications, Crit. Rev. Solid State Mater. Sci. 26 (2001) 145–249.
[2] Y. Li, X. Li, R. He, J. Zhu, Z. Deng, Artificial lamellar mesostructures to WS_2 nanotubes, J. Am. Chem. Soc. 124 (2002) 1411–1416.
[3] T. Kasuga, M. Hiramatsu, A. Hoson, T. Sekino, K. Niihara, Formation of titanium oxide nanotube, Langmuir 14 (1998) 3160–3163.
[4] T. Kasuga, M. Hiramatsu, A. Hoson, T. Sekino, K. Niihara, Titania nanotubes prepared by chemical processing, Adv. Mater. 11 (1999) 1307–1311.
[5] Y.Q. Wang, G.Q. Hu, X.F. Duan, H.L. Sun, Q.K. Xue, Microstructure and formation mechanism of titanium dioxide nanotubes, Chem. Phys. Lett. 365 (2002) 427–431.
[6] X. Sun, Y. Li, Synthesis and characterization of ion-exchangeable titanate nanotubes, Chem. Euro. J. 9 (2003) 2229–2238.
[7] R. Yoshida, Y. Suzuki, S. Yoshikawa, Effects of synthetic conditions and heat-treatment on the structure of partially ion-exchanged titanate nanotubes, Mater. Chem. Phys. 91 (2005) 409–416.
[8] T. Kasuga, Formation of titanium oxide nanotubes using chemical treatments and their characteristic properties, Thin Solid Films 496 (2006) 141–145.
[9] L.Q. Weng, S.H. Song, S. Hodgson, A. Baker, J. Yu, Synthesis and characterisation of nanotubular titanates and titania, J. Eur. Ceram. Soc. 26 (2006) 1405–1409.
[10] J. Yu, H. Yu, B. Cheng, C. Trapalis, Effects of calcination temperature on the microstructures and photocatalytic activity of titanate nanotubes, J. Mol. Catal. A: Chem. 249 (2006) 135–142.
[11] D.S. Seo, J.K. Lee, H. Kim, Preparation of nanotube-shaped TiO_2 powder, J. Cryst. Growth 229 (2001) 428–432.
[12] A. Cassano, R. Molinari, M. Romano, E. Drioli, Treatment of aqueous effluents of the leather industry by membrane processes: a review, J. Membr. Sci. 181 (2001) 111–126.
[13] N.D. Lourenco, J.M. Novais, H.M. Pinheiro, Effect of some operational parameters on textile dye biodegradation in a sequential batch reactor, J. Biotechnol. 89 (2001) 163–174.
[14] Z. Sun, Y. Chen, Q. Ke, Y. Yang, J. Yuan, Photocatalytic degradation of a cationic azo dye by TiO_2/bentonite nanocomposite, J. Photochem. Photobiol. A: Chem. 149 (2002) 169–174.
[15] C.C. Wang, L.C. Juang, T.C. Hsu, C.K. Lee, J.F. Lee, F.C. Huang, Adsorption of basic dyes onto montmorillonite, J. Colloid Interf. Sci. 273 (2004) 80–86.
[16] A. Andrzejewska, A. Krysztafkiewicz, T. Jesionowski, Treatment of textile dye wastewater using modified silica, Dyes Pigments 75 (2007) 116–124.
[17] A. Andrzejewska, A. Krysztafkiewicz, T. Jesionowski, Adsorption of organic dyes on the aminosilane modified TiO_2 surface, Dyes Pigments 62 (2004) 121–130.
[18] G. Crini, Non-conventional low-cost adsorbents for dye removal: a review, Bioresour. Technol. 97 (2006) 1061–1085.
[19] K.R. Ramakrishna, T. Viraraghavan, Dye removal using low cost adsorbents, Water Sci. Technol. 36 (1997) 189–196.
[20] G. Annadurai, R.S. Juang, D.J. Lee, Use of cellulose-based wastes for adsorption of dyes from aqueous solutions, J. Hazard. Mater. B92 (2002) 263–274.
[21] T. Robinson, B. Chandran, P. Nigam, Removal of dyes from an artificial textile dye effluent by two agricultural waste residues, corncob and barley Husk, Environ. Int. 28 (2002) 29–33.
[22] C.C. Wang, L.C. Juang, C.K. Lee, T.C. Hsu, J.F. Lee, H.P. Chao, Effects of exchanged surfactant cations on the pore structure and adsorption characteristics of montmorillonite, J. Colloid Interf. Sci. 280 (2004) 27–35.
[23] M.M. Mohamed, Acid dye removal: comparison of surfactant-modified mesoporous FSM-16 with activated carbon derived from rice husk, J. Colloid Interf. Sci. 272 (2004) 28–34.
[24] S. Wang, H. Li, L. Xu, Application of zeolite MCM-22 for basic dye removal from wastewater, J. Colloid Interf. Sci. 295 (2006) 71–78.
[25] K.Y. Ho, G. McKay, K.L. Yeung, Selective adsorbents from ordered mesoporous silica, Langmuir 19 (2003) 3019–3024.

[26] L.C. Juang, C.C. Wang, C.K. Lee, Adsorption of basic dyes onto MCM-41, Chemosphere 64 (2006) 1920–1928.
[27] S.H. Lin, R.S. Juang, Heavy metal removal from water by sorption using surfactant-modified montmorillonite, J. Hazard. Mater. B92 (2002) 315–326.
[28] D.M. Ruthven, Principles of Adsorption and Adsorption Processes, Wiley, New York, 1984, p. 44.
[29] S. Azizian, Kinetic models of sorption: a theoretical analysis, J. Colloid Interf. Sci. 276 (2004) 47–52.
[30] G.E. Boyd, A.W. Adamson, L.S. Myers Jr., The exchange adsorption of ions from aqueous solutions by organic zeolites. II. Kinetics, J. Am. Chem. Soc. 69 (1947) 2836–2848.
[31] V. Vadivelan, K.V. Kumar, Equilibrium, kinetics, mechanism, and process design for the sorption of methylene blue onto rice husk, J. Colloid Interf. Sci. 286 (2005) 90–100.
[32] J. Yu, H. Yu, B. Cheng, X. Zhao, Q. Zhang, Preparation and photocatalytic activity of mesoporous anatase TiO_2 nanofibers by a hydrothermal method, J. Photochem. Photobiol. A: Chem. 182 (2006) 121–127.
[33] S. Brunauer, The Adsorption of Gases and Vapours, Oxford University Press, 1944.
[34] F. Helfferich, Ion Exchange, McGraw-Hill, New York, 1962, p. 166.
[35] K.P. Sing, D. Mohan, S. Sinha, G.S. Tondon, D. Gosh, Color removal from wastewater using low-cost activated carbon derived from agricultural waste material, Ind. Eng. Chem. Res. 42 (2003) 1965–1976.
[36] K.V. Kumar, V. Ramamurthi, S. Sivanesan, Modeling the mechanism involved during the sorption of methylene blue onto fly ash, J. Colloid Interf. Sci. 284 (2005) 14–21.
[37] S. Wang, H. Li, S. Xie, S. Liu, L. Xu, Physical and chemical regeneration of zeolitic adsorbents for dye removal in wastewater treatment, Chemosphere 65 (2006) 82–87.
[38] S.G. Huling, P.K. Jones, W.P. Ela, R.G. Arnold, Fenton-driven chemical regeneration of MTBE-spent GAC, Water Res. 39 (2005) 2145–2153.
[39] H. Zhu, X. Gao, Y. Lan, D. Song, Y. Xi, J. Zhao, Hydrogen titanate nanofibers covered with anatase nanocrystals: a delicate structure achieved by the wet chemistry reaction of the titanate nanofibers, J. Am. Chem. Soc. 126 (2004) 8380–8381.